AADE-25-NTCE-043

Method Development to Evaluate Wellbore Instability of Mid- to Deep-Shale Formations

Nancy Zhou, Meng Lu, Janine Shipman, Steven Vaughan, Tim Dunne, Daneil Gardea, and Jiaxiang Ren, CNPC USA;
Jing Hu, and Fengfeng Xiao, CNPC Chuanqing Drilling Engineering Co., Ltd. Drilling Fluid Technical Service Company

Abstract

To improve wellbore stability during the drilling of mid- to deep-shale formations, it is essential to identify the causes of the wellbore instability. Systematic experimental work was implemented to develop methods for investigating reasons of instability and to screen drilling fluid additives for improving the stability using drilled cuttings from the field.

Drilled cuttings were analyzed by X-ray diffraction (XRD) to find their mineralogy and clay compositions. To evaluate the hydration potential of shale, we crushed and compacted shale cuttings to wafers for linear swell tests (LST) under temperature and pressure of the targeted shale formations. Selected cuttings were polished and then prepared as shale assemblies. Microstructural analyses using optic microscopy were conducted to gain an understanding of microfracture width, length, and depth of shale samples before infiltration test.

Infiltration tests were performed using a modified flexible wall permeameter first and then a high temperature high pressure (HTHP) permeability plugging apparatus (PPA). Several commercially available 'sealing and plugging agents' (SPAs) were injected into shale samples using the infiltration setup by flowing SPA dispersions through the shale under certain pressures. Comparing infiltration rates and breakthrough pressures, we screened SPAs to improve the wellbore instability. The difference of infiltration rate between the untreated and the SPA-treated shale sample was significant.

Our experimental work introduced an accessory (shale assembly) to the well-known lab equipment of PPA. Moreover, using easily accessible drilled cuttings to create shale assemblies, instead of ceramic disc, resulted in more practical outcomes.

Introduction

Mid- to deep-shale formations are formations with shale rock having depth over 5000 ft. Mid-deep shale reservoirs are currently the principal target interval for global development. Deep shale formations have enormous resource potential in China, accounting for over 50% of total resources. With the depth increasing, the pore pressure and temperature of shale formation increase. Besides the challenges with hotter temperature and higher pressure, other challenges from complex geologic heterogeneity of shale and wellbore instability issues from reactive clays that can swell are critical to consider during the drilling fluid design stage. The deep shale gas reservoirs of the Wufeng-Longmaxi formations in the southern Sichuan Basin exhibit strong heterogeneity and complex geological characteristics (Li et al., 2023): X-ray analysis has shown the quartz and clay minerals are the two main compositions with 32 to 78 wt%, and 4 to 51 wt%, respectively.

There are a lot of factors influencing the wellbore instability during the drilling process, particularly for shale formation or high over balance conditions. These factors can be mechanical, chemical, or a combination of both. In specific fields, certain factor(s) dominate. For example, fractured shale formation is more susceptible to wellbore collapse or fluid invasion that leads to drilling fluid loss if an effective filter cake does not form. SPAs with different particle sizes and chemistry are typically added to drilling fluids (Goud et al., 2006, Yan et al., 2015, Musa et al., 2022) to control fluid invasion and strengthen the wellbore of shale formations.

Currently, there is no official recommended method to evaluate the efficiency of the sealing and plugging treatments for shale drilling. Several laboratory procedures are used for additive screening, such as the shale particle dispersion test and the dynamic filtration test (Faraz Khan et al., 2024). Additionally, specialized downhole condition evaluation devices, such as the pressure transmission test (van Oort, 1994), have been employed over the years to assess drilling fluids in terms of wellbore instability (Stowe et al., 2001; Akhtarmanesh et al., 2013; van Oort et al., 2016; Khramov et al., 2023). While basic screening tests are simple to conduct, they provide limited information (Khramov et al., 2023). In contrast, downhole evaluation devices are expensive and often require core plugs, which are not always easily accessible, such as those measuring 2.54 cm in diameter and 5 cm in length (Li, 2020) for triaxial and stress tests.

Infiltration tests were initially designed to inject nanoparticles into shale samples at an inflow pressure of approximately 120 psi (Zhou et al., 2020). Later, it was discovered that infiltration tests using a modified flexible wall permeameter could be used to rank the plugging efficiency of

SPAs (Zhou et al., 2024). The infiltration curves revealed different stages, including an unplugged stage, a plugged stage, and, in some cases, a breakthrough of the plugged stage with various SPAs observed.

The goal of our project is to develop a water-based drilling fluid (WBDF) for mid- to deep-shale formations, addressing both environmental and economic concerns. Currently, oil-based drilling fluid (OBDF) is used in the field but is associated with lost circulation issues. While OBDF offers advantages in shale stabilization, lubricity, and contamination tolerance (Rady et al., 2024), it has no effectiveness in sealing and plugging fractures to prevent lost circulation if no sealing and plugging agents are added. This paper presents our experimental work aimed at identifying the true causes of wellbore instability in targeted mid- to deep-shale formations. Additionally, we evaluate several commercially available SPAs to determine their ability to seal natural fractures or prevent fracture propagation, ultimately improving wellbore instability.

Materials and methodology

Materials

Shale samples were collected from well sites in two different fields. We picked the big pieces for infiltration tests (See Figure 1) and smaller ones, less than 2 mm, that passed through size 10 sieve, for LST and XRD. In Figure 1, samples A, seen in Figure (a), and B, seen in Figure (b), were from one field with the reservoir vertical depth from 6,800 to 12,700 ft, a mid- to deep-shale formation. Sample C, seen in Figure (c), was from the other field with a total depth of 22,000 ft, and vertical depth of 14,360 ft. Sample A was labeled as caving chips. The width of sample A varies from 3 cm to 5 cm. The length of sample A varies between 3 cm to 7 cm. The thickness of sample A varies from 0.5-1 cm. Samples B and C were labeled as horizontal shale cuttings. The shape of them is irregular and sizes are smaller than those of sample A.

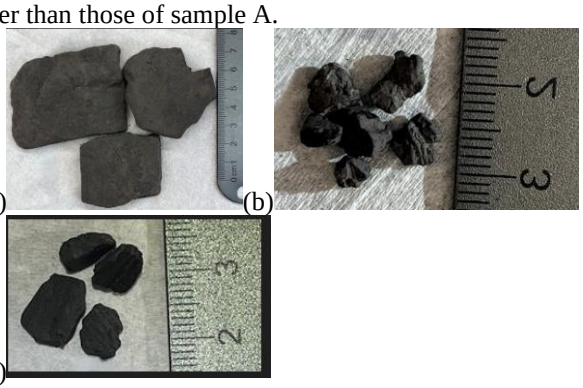

Figure 1 – Caving shale chips (Sample A) and shale cuttings (Samples B and C).

The sealing and plugging agents discussed in this paper are commercially available products, see Table 1 for their physical properties. Two liquid samples are in water media, one sample is solid in powder form.

Table 1 Physical properties of SPAs.

SPA	Appearance
NZ76-25B	white emulsion liquid
NZ76-25C	black liquid
NZ76-25F	solid

Linear swell testing

The Linear Swell Test (LST) was used to evaluate shale hydration by measuring the expansion of reconstituted shale wafers over time. These wafers were prepared from shale cuttings by grinding and compacting small particles (less than 2 mm after sieving) of shale samples B and C. The tests were conducted under simulated downhole conditions, high temperature (~150°C/302°F) and high pressure (up to 10,000 psi), using a HPHT Rheometer equipped with the manufacturer's Linear Swell Meter Module. Deionized (DI) water was used as the saturating fluid to assess the maximum potential hydration of shale samples.

Microfracture characterization

Before conducting infiltration tests, the polished top and bottom surfaces of the shale assemblies were examined using a high-resolution digital optical microscope. Two lenses were utilized for this analysis: the ZS-20, offering magnification ranges from 20x to 200x, and the ZS-200, covering 200x to 2000x magnification. Initial full-view images of the shale samples were captured with the ZS-20 lens to center the microscope and scan for fractures. Upon identifying fractures, the microscope's "plane measurement" feature was employed to determine both the length and width of the cracks. For more detailed analysis, higher magnifications (200x or greater) were applied using the ZS-200 lens. The fracture depth was measured by enabling the use of the microscope's 3D capabilities at a higher magnification.

Infiltration test

Infiltration tests were conducted using the modified flexible wall permeameter and then a permeability plugging apparatus. During the infiltration test, SPAs were dispersed into a brine (e.g. 10% KCl in water) to form a liquid suspension. The suspension was thoroughly homogenized via mixing and then dispersed using an ultrasonic blender. After that, for infiltration tests using the modified flexible wall permeameter (Zhou et al., 2020), the SPA suspension was loaded into the double acting cylinder, see Figure 2 (a). It was then injected from the double acting cylinder to the small cap and filled the entire space of the top surface of the shale sample, see Figure 2 (b). The green arrow indicates the direction in which the SPA suspension flows as seen in Figure 2 (c). Before the injection, all shale assemblies were rehydrated by placing them in the dedicators above a synthetic pore fluid solution (brine) until no more weight changes were observed. Injection pressures of less than 130 psi, e.g. 500 kPa, were used and confining pressures, less than 150 psi, e.g. 700 kPa, were selected. The exit flow was

collected in a glass flask. The cumulative injection volume was recorded over time. The infiltration test using the modified flexible wall permeameter is limited in pressure and temperature due to the materials used in its construction.

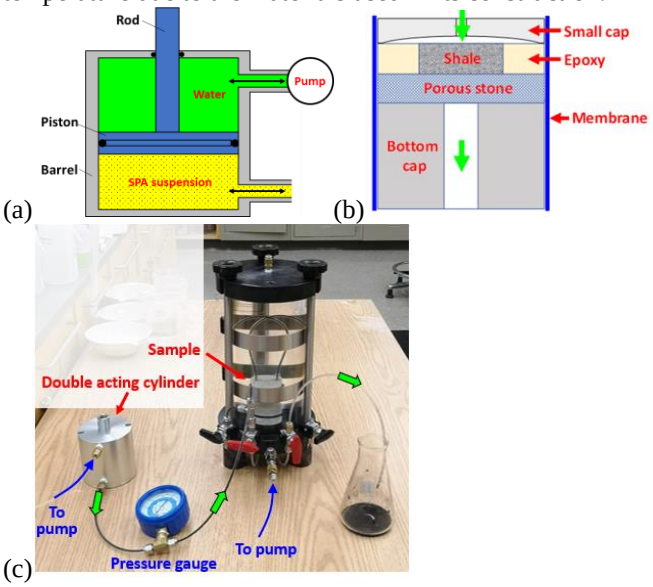

Figure 2 – Infiltration test using the modified flexible wall permeameter: (a) section diagram of the double acting cylinder, (b) sample part, and (c) test setup.

Infiltration test method using the permeability plugging apparatus (PPA) was developed by replacing the ceramic discs with shale assemblies. The shale assembly was soaked in brine to rehydrate before running an infiltration test. The goal of using the PPA is to improve the pressure and temperature limitation of modified flexible wall permeameters. Shale assemblies were prepared using big pieces of sample A, B and C, as shown in Figure 1. The permeability of the shale sample was then tested by applying brine or base fluid to the shale assembly using a high-pressure pump to control the injection pressure. When a SPA is added into the fluid, the sealing and plugging effect is determined by comparing the filtrate collection rate and breakthrough pressure, if observed.

Results and Discussions

Drilled cuttings characterization

Shale samples A, B, and C range in color from black to dark gray and gray. Their mineralogical composition was characterized using X-ray diffraction (XRD). Table 2 summarizes the whole-rock mineralogy (a) and clay mineral composition (b). Quartz is the most abundant mineral, comprising 38.0% to 54.0% of the samples. Clay minerals, ranging from 20.1% to 31.5%, are the second most abundant group. Quartz and feldspar are classified as framework silicates, while other identified minerals include pyrite, sulfate minerals, rutile, and barite. The relatively high carbonate content in these rocks suggests potential for acidizing to enhance production, as well as the possibility of chemical reactions that could reduce wellbore stability.

Table 2 Mineralogical and clay contents of shale samples characterized by XRD: (a) whole rock mineralogy, (b) clay mineralogy.

(a)

Sample	Quartz	Feldspar	Carbonate	Clay	Others
A	46.6	6.9	11.3	26.8	7.9
B	38.0	6.0	13.0	31.5	11.6
C	54.0	8.4	10.3	20.1	7.3

(b)

Sample	Smectite	I/S	Illite+Mica	Kaolinite	Chlorite
A	0.0	0.0	18.1	4.0	4.7
B	0.0	0.0	26.3	0.0	5.2
C	0.0	0.0	15.8	1.6	2.7

The clay mineral analysis in Table 2(b) indicates the absence of smectite and Illite/Smectite (I/S) mixed-layer minerals, confirming that the shale lacks expandable properties. Consequently, this formation is a strong candidate for the use of water-based drilling fluids.

Two shale samples, B and C, with the highest and the lowest clay minerals contents, were selected to determine shale hydration potential. They were dried, ground, and then pressed into pellets. The pellet was placed in the LSM Module with DI water as the fluid. The method was run and the data was acquired accordingly.

The swelling was averaged approximately 2% for sample B as shown in Figure 3(a) for bottomhole pressures of 5000 psi and 10000 psi. While sample C has swelling average approximately 3% as shown in Figure 3(b). For both shale samples, swelling percentages decreased slightly as pressure increased. All swelling results are relative small, at 2% and 3% respectively, indicating a low hydration potential. They are significantly lower compared to typical swelling or expandable shales, which often exhibit swelling exceeding 15%. We conclude that the hydration of the shale will not induce wellbore instability for this target field. Again, our targeted shale formation should be a suitable candidate for using water-based drilling fluids.

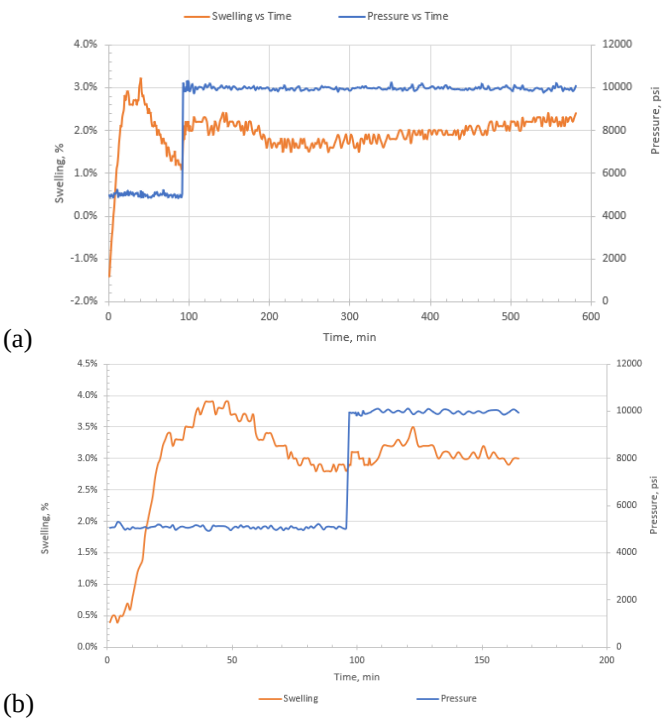

Figure 3 – LST results of shale samples, B and C.

The digital microscope enables clear observation of surface details and precise measurement of observed features. Seven pieces of shale sample A were prepared into shale assemblies TD-1, SV-1 through SV-6 for infiltration tests using a permeability plugging apparatus (PPA). Figure 4 shows: (a) the surface image of TD-1, (b) the width measurement of fractures in SV-5, and (c) the depth measurement of fractures in SV-5.

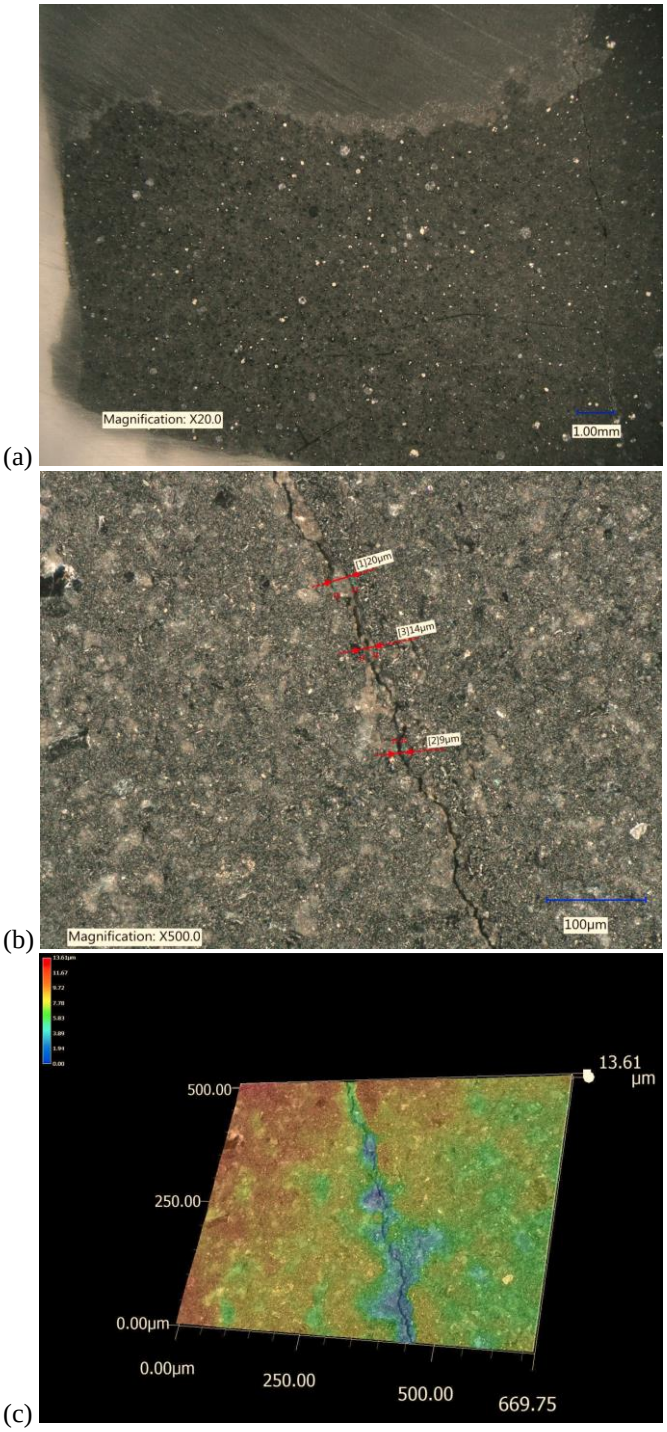

Figure 4 – Microscopic images of shale samples.

Table 3 summarizes the width, length and depth of fractures found in all seven shale samples. The much wider fractures was found for shale disc SV-3 and TD-1. The much longer fractures was found for shale disc SV-5 and SV-6. The much deeper fractures was found for shale disc TD-1 and SV-5. More than 10 fractures were identified on both sides of SV-6, while only 2 fractures were found in SV-3. The presence of numerous fractures explains the observed drilling fluid loss in the field,

which is most likely due to fractures, whether natural or induced. Additionally, the filtrate loss into the wellbore may further destabilize the wellbore, leading to large caving chips being collected in the shaker.

Table 3 Summary of fracture width, length and depth for all seven shale samples.

Shale Sample	TD-1	SV-1	SV-2	SV-3	SV-4	SV-5	SV-6
Width, µm	22-370	5-15	5-15	300-500	3-52	4-24	22-26
Length, µm	30-420	20-60	500-1000	800-1300	1500-2500	6000-12000	4000-8000
Depth, µm	78-230	10-50	9-40	10-45	9-22	14-112	6-40

Infiltration Tests
Using modified flexible wall permeameter

SPA suspensions were prepared by adding an SPA sample to brine, specifically 10 wt.% KCl solution, to prepare 5% activity of the SPA. This mixture was initially stirred magnetically at 1000 rpm for 1 min, followed by high-speed blending at 19,000 rpm for 10 min to ensure a uniform suspension solution. The freshly prepared solutions were immediately injected into highly polished and hydrated shale assembly. This setup ensured that the SPA suspension could only permeate into and through the micropores and microfractures of the shale specimen, without affecting the embedding epoxy resin. For more details, refer to Zhou et al., 2020.

The largest piece of sample A collected was selected to prepare four shale assemblies, labeled A1 to A4, for infiltration tests using a modified flexible wall permeameter. Table 4 summarizes the two infiltration tests using injection pressure 500 kPa (72.5 psi) for two specimens discussed in this paper. The infiltration tests of IT-1 and IT-2 were designed to evaluate the selected commercial SPA sample NZ76-25F. For IT-1, 10% KCl solution was injected, and the result from IT-1 will serve as the baseline for IT-2. It is assumed that both specimens, being made from the same piece of shale sample A, should exhibit the same permeability.

Table 4 Summary of infiltration tests using modified flexible wall permeameter.

Test#	Shale assembly	SPA	Solution injected
IT-1	A2	none	10% KCl Water
IT-2	A4	NZ76-25F	SPA solution in 10% KCl solution

Figure 5 shows infiltration results of the 10% KCl solution injection alone into Sample A shale assembly (A2). The dark blue curve recorded the temperature changes overtime. This infiltration test took over 23 days. The red curve displays the history of the injected volumes. Less than 1.0 mL of a final volume was injected. Because the infiltration red injection curve fluctuates periodically with a negative correlation to the temperature log (in blue), we concluded that this fluctuation of injected volumes is caused by temperature changes during the test (Zhou et al., 2020). Due to the very low permeability of shale, temperature variation (or thermal change) alters the volumes of the tubes, pumps, cell, and the suspension, and this influence would be particularly significant for the volume measurements while testing super-low-permeability shales.

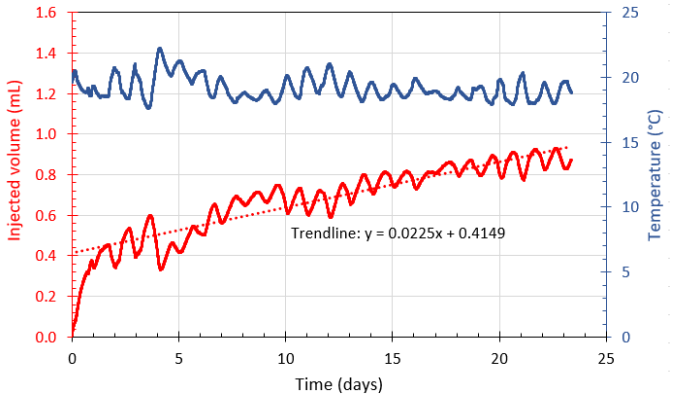

Figure 5 – Infiltration results of IT-1 using 10% KCl solution.

Figure 6 shows infiltration results of IT-2 with the recording of injected volumes of suspensions of NZ76-25F versus time. Three stages were observed for the whole injection process. At the beginning of the infiltration process, the injected volumes increased with a slope of 0.8201 mL/d for the first day. Because of the sealing effect of NZ76-25F, some fractures and flow channels were sealed, that reduced the injection slope from 0.8201 mL/d to 0.3415 mL/d (decreasing 58%) from 2nd to 4th days, respectively. And then the fractures and flow channels are totally plugged, a negative slope or almost no slope was observed. Comparing the injection slope of Figure 5 (0.0225 mL/d) with those from Figure 6, we concluded that: 1) NZ76-25F has significant plugging effects; 2) specimens made from the same piece of shale sample A do not necessarily have the same permeability, indicating that shale sample A is highly heterogeneous.

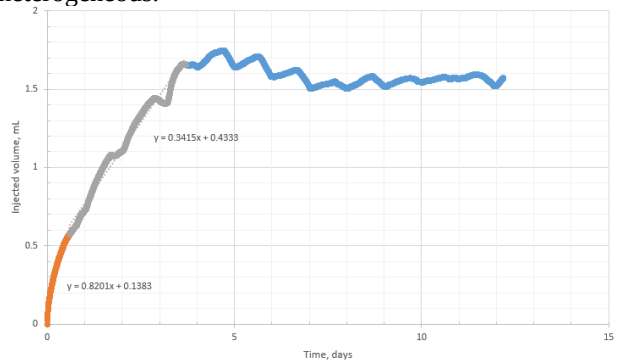

Figure 6 – Infiltration results of IT-2 using suspensions of NZ76-25F.

Using permeability plugging apparatus

Considering the limitation of the modified flexible wall permeameter on temperature and pressure, we developed the infiltration method using permeability plugging apparatus (PPA). PPA is used widely in the drilling fluid industry for permeability plugging tests (PPT) to evaluate lost circulation material or filtration agents. API establishes the designations of ceramic discs with mean pore throat diameter ranging from 10 µm to 120 µm. Those diameters are significantly larger than the pore throats of typical shale formations and do not encompass the full range of fracture sizes measured in Table 3. Therefore, the current PPT method cannot be used for sealing and plugging

effect evaluation of SPAs that are potentially used for our targeted shale formation drilling.

The modification involved using shale assemblies to replace the ceramic discs. A total of seven shale assemblies were prepared, all made from caving shale chips, as shown in Figure 1A. The first step is to test the original permeability of shale samples using KCl solution (KCLS) as the injection fluid. KCLS was prepared by dissolving 100 g of potassium chloride (ACS agent grade) in 900 mL of DI water. The test pressure for the permeability check was set to 60 psi (414 kPa). Under this pressure, a higher injection rate (the slop of filtrate volume verse time) indicates a higher permeability. Table 5 presents the results of infiltration tests using KCLS. "ND" indicates that no detectable filtrate was collected within 30 min with a pressure of 60 psi. Three shale samples, SV-1, SV-2 and SV-3, showed ND results for the infiltration test using KCLS. The remaining four shale samples had infiltration rates ranging from 0.18 to 2.95 mL/min. Those highlight the heterogeneity of shale chips.

Table 5 Summary of KCLS infiltration test results.

Shale Sample	TD-1	SV-1	SV-2	SV-3	SV-4	SV-5	SV-6
Slope of KCls	0.9657	ND	ND	ND	2.9427	2.179	0.1827

Infiltration tests from modified permeability plugging apparatus (IT-MPPA) were summarized in Table 6. The volume collected is the filtrate volume. The filtrate volume collection rate should be positively related to the permeability of shale according to Darcy's law.

Table 6 Summary of IT-MPPA.

Test#	Shale Sample	SPA evaluated
IT-MPPA-1	TD-1	NZ76-25C
IT-MPPA-2	SV-5	NZ76-25B
IT-MPPA-3	SV-6	NZ76-25F

Figure 7 shows the infiltration results of IT-MPPA-1, using shale assembly of TD-1 and SPA solution of NZ76-25C. In the filtration volume curve, sequential slope changes were observed: first during the injection of 10% KCl solution (KCLS, gray line with a linear trendline), followed by the injection of the SPA solution of NZ76-25C (ABT-SPA, yellow line with a linear trendline), and finally, the injection of 10% KCl solution after the SPA solution (ABT-KCLS, blue line with a linear trendline). The slopes were 0.9657 mL/min, 0.1376 mL/min, and 0.0343 mL/min, respectively. The decreasing slope indicates the sealing effect of NZ76-25C. The blue flat lines represent complete plugging with no fluid passing through. NZ76-25C temporarily plugged the shale sample TD-1 for over 100 min before the liquid breakthrough. The breakthrough pressure was 120 psi.

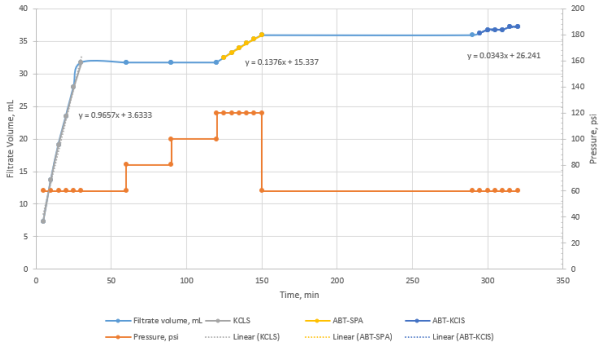

Figure 7 – Infiltration results of IT-MPPA-1 using NZ76-25C.

Shale assembly of SV-6 was used to evaluate the sealing and plugging effect of SPA NZ76-25F. The results of the infiltration test of IT-MPPA-2 are shown in Figure 8. There has been no filtrate collected for 3 hours at 60 psi. There was no filtrate observed when pressure was increased to 120 psi for 30 min, 200 psi for 30 min, 300 psi for 30 min. This demonstrates the plugging effect of NZ76-25F. When the pressure reached 400 psi, filtrate was observed, also indicating a breakthrough. The breakthrough pressure for sealing agent NZ76-25F is 400 psi. Given its higher breakthrough pressure and longer plugged stage, NZ76-25F is ranked as having a better plugging effect than NZ76-25C.

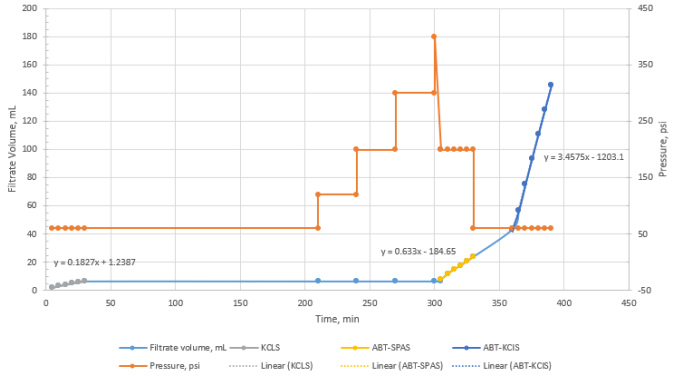

Figure 8 – Infiltration results of IT-MPPA-2 using NZ76-25F.

Another sealing agent, NZ76-25B, was tested using the modified PPA with the shale assembly of SV-5. SV-5 exhibited a much larger slope of KCLS, 2.179 mL/min, compared to SV-6, which had a slope of 0.1827 mL/min. Figure 9 shows the KCl solution injection followed by the SPA solution of NZ76-25B injection. During the NZ76-25B solution injection, the pressure was increased and held for 30 mins at each pressure step (60, 120, 200, 300, 400, 500, 600 and 700 psi). No filtrate was observed during this solution injection sequence. The pressure was then held at 700 psi for additional 4 hours, no filtration was observed. This demonstrates the plugging effect of NZ76-25B! It can withstand pressures up to 700 psi for more than 4 hours. Given the highest breakthrough pressure and the longest plugged stage, we rank NZ76-25B as the best SPA of our testing SPAs.

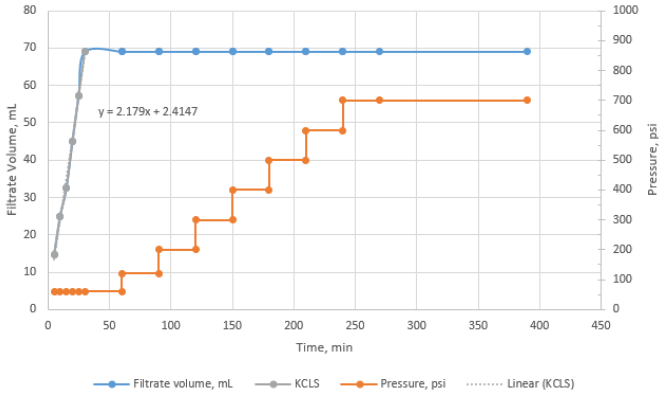

Figure 9 – Infiltration results of IT-MPPA-3 using NZ76-25B.

Conclusions

In summary, to evaluate wellbore instability of a specify of mid- to deep-shale formations and screening SPA to prevent/stop loss circulation, a method was developed through systematic experimental work on drilled cuttings. This method includes the steps below.

(1) Collect drilled cuttings from a field having wellbore instability issues.

(2) Perform XRD analysis to find minerology and clay compositions of the drilled cuttings.

(3) Conduct LST under temperature and pressure conditions of the shale formations.

(4) Examine fractures using a digital microscope.

(5) Prepare shale assembly using drilled cuttings to replace ceramic discs in the PPA.

(6) Run infiltration tests with the base brine solution and the suspension solution of SPA.

(7) Analyze infiltration test results and rank performance based on the sealing and plugging effect.

8) Submitted recommendation to field engineers to improve the wellbore instability.

In the next phase, we plan to conduct high-temperature infiltration tests using PPA.

Acknowledgments

The authors would like to acknowledge CNPC USA for granting permission to publish this paper. Special thanks are extended to Wei Sun and Guoping Zhang of the University of Massachusetts Amherst for their valuable assistance with some XRD analysis and the infiltration tests using the modified flexible wall permeameter.

Nomenclature

API	=	*America Petroleum Institute*
µm	=	*Micrometer*
ACS	=	*American Chemical Society*
DI	=	*de-ionized*
ft	=	*feet*
g	=	*gram*
hrs	=	*Hours*
HTHP	=	*high temperature high pressure*
I/S	=	*Illite/Smectite*
IT	=	*Infiltration test*
IT-MPPA	=	*Infiltration tests from modified permeability plugging apparatus*
KCl	=	*Potassium chloride*
KCLS	=	*KCl solution*
kPa	=	*kilopascal*
LST	=	*linear swell tests*
min	=	*Minute*
mL	=	*Mililiter*
OBDF	=	*oil-based drilling fluid*
PPA	=	*permeability plugging apparatus*
PPT	=	*Permeability plugging test*
psi	=	*Pounds per square inch*
rpm	=	*Revolutions per minute*
SPA	=	*Sealing and plugging agent(s)*
WBDF	=	*water-based drilling fluid*
wt%	=	*weight percent*
XRD	=	*X-ray diffraction*

References

Akhtarmanesh S., Ameri Shahrabi, M. J., Atashnezhad, A. 2013. "Improvement of wellbore stability in shale using nanoparticles." Journal of Petroleum Science and Engineering,Volume 112, December 2013, Pages 290-295. https://doi.org/10.1016/j.petrol.2013.11.017

Goud, M.C., Joseph, G. 2006. "Drilling Fluid Additives and Engineering to Improve Formation Integrity." SPE/IADC Indian Drilling Technology Conference and Exhibition, Mumbai, India, October 2006. SPE-104002-MS. https://doi.org/10.2118/104002-MS

Khramov, D., Panamarathupalayam, B., Barmatov, E. 2023. "Research, Evaluation of Laboratory Performance Tests for Drilling Fluids." AADE-23-FTCE-012. AADE Fluids Technical Conference and Exhibition, Midland, Texas, April 4-5, 2023. Available from https://www.aade.org

Li, J., Li, H., Yang, C., Ren, X. R., and Li, Y. 2023. "Geological Characteristics of Deep Shale Gas and Their Effects on Shale Fracability in the Wufeng-Longmaxi Formations of the Southern Sichuan Basin, China." Applied Sciences 13 (24): 13194. https://doi.org/10.3390/app132413194

Li, Y. 2020. "Mechanics and Fracturing Techniques of Deep Shale from the Sichuan Basin, SW China." Energy Geoscience 2 (2021) 1-9. https://doi.org/10.1016/j.engeos.2020.06.002

M. F. K., Z.Karajagi, V.Pradet, F.Molina, D.Ahuir, N.Yahyono, A.Addagalla, V.Cho, A.Gad, "Stabilizing the Complex Ultra Extended Reach Depleted Reservoir Wellbores Using Nano Particles in Water Base Mud System". AADE-24-FTCE-008, AADE National Technical Conference, Houston, April 16–17, 2024. Available from www.aade.org.

Musa, I., Hale, A., Mohandes, M. E. 2022. "Wellbore Strengthening – Continuous Application or Sweep as Needed?" AADE-22-FTCE-068, AADE Fluids Technical Conference and Exhibition, Houston, Texas, April 19-20, 2022. Available from https://www.aade.org

Stowe, C., Halliday, W., Xiang, T., Clapper, D., Morton, K., Hartman, S. 2001. "Laboratory Pore Pressure Transmission Testing of Shale." AADE 01-NC-HO-44, AADE 2001 National Drilling Conference, "Drilling Technology- The Next 100 years", held at the Omni in Houston, Texas, March 27 - 29, 2001. Available from https://www.aade.org

van Oort, E., Hoxha, B.B., Hale, A. 2016. " How to Test Fluids for Shale compatibility." AADE-16-FTCE-77, Available from

https://www.aade.org

Yan, L., Li, C., Zhang, Z., Wang, J., Xu, X., Sun, J., Su, Y. 2015. "Successful Application of Unique High-Density Water-Based Drilling Fluid Used in Zhaotong Shale Gas Horizontal Wells." SPE/IATMI Asia Pacific Oil & Gas Conference and Exhibition, Nusa Dua, Bali, Indonesia, October 2015. SPE-176428-MS, https://doi.org/10.2118/176428-MS

Zhou, N., Qu, Y., Geng, Y., Lu, M., Shipman, J., Liu, F., Yan, S., and Zhang, G. 2024. "A Nanoindentation Method to Evaluate Sealing and Plugging Agents Used in Water-Based Drilling Fluids for Shale Formations." AADE-24-FTCE-028, AADE National Technical Conference, Houston, April 16–17, 2024. Available from www.aade.org.

Zhou, N., Wu, Y., Lu, M., Li, Y., Liu, F. Zhang, G. 2020. "An Experimental Study to Demonstrate That Nanoparticles Can Filter into Shale Formations and Improve Wellbore Stability." Abu Dhabi International Petroleum Exhibition & Conference, Abu Dhabi, UAE, Nov 9-12, 2020. SPE-202754-MS. https://doi.org/10.2118/202754-MS.